Mechanistic Study of the Oxidative Degradation of the Triazole Antifungal Agent CS-758 in an Amorphous Form

EIJI UEYAMA,[1] NOBUYUKI SUZUKI,[1] KENJI KANO[2]

[1]Analytical and Quality Evaluation Research Laboratories, Pharmaceutical Technology Division, Daiichi Sankyo, Hiratsuka, Kanagawa 254-0014, Japan

[2]Division of Applied Life Sciences Graduate School of Agriculture, Kyoto University, Kitashirakawa Oiwake-cho, Kyoto 606-8502, Japan

Received 12 June 2012; revised 13 September 2012;

Published online 5 October 2012 in Wiley Online Library (wileyonlinelibrary.com). DOI 10.1002/jps.23339

ABSTRACT: In this study, the degradates generated from a pharmaceutical solid were characterized, and a mechanistic pathway underlying their formation was proposed. The chemical stability of a novel triazole antifungal drug, CS-758, deteriorated significantly when the crystal was disordered, and characteristic degradates were generated. A total of eight degradates in solution and nine degradates in a solid state were isolated by preparative liquid chromatography. Degradates were characterized using high-performance liquid chromatography–photodiode array, mass spectrometry, and nuclear magnetic resonance. Radical-mediated oxidation is proposed as the main degradation pathway in the solid state. The initiation step of this pathway is hydrogen atom abstraction from a methine carbon that is adjacent to a dien moiety and the formation of a delocalized vinylic radical intermediate. Molecular oxygen is then added to the radical position to form hydroperoxides. There are three potential oxidation routes based on the proposed autoxidation pathway that lead to the generation of the dioxane ring-opening hydroxyl form, the 9,10-epoxide form, or the 11,12-epoxide form, depending on the substituted position of the added molecular oxygen. The epimer compound generated via the vinylic radical intermediate and sulfoxides was characterized. This degradation mechanism provides the scientific foundation for an oxidative stressing system currently under investigation. © 2012 Wiley Periodicals, Inc. and the American Pharmacists Association J Pharm Sci 102:104–113, 2013

Keywords: oxidation; amorphous; solid state; stability; chemical stability; degradation products

INTRODUCTION

In addition to hydrolysis, oxidation is a major pathway of drug degradation. Several different types of oxidation mechanisms are known, such as autoxidation (mediated by free radicals),[1,2] nucleophilic/electrophilic oxidation (mediated by peroxides),[3,4] electron transfer oxidation (mediated by transition metals),[5] and photochemically induced oxidation (singlet oxidation, etc.).[6,7] In some cases, an oxidation reaction is triggered by trace amounts of impurities (e.g., peroxides or transition metals) contaminating the drug excipients[3–5] or by the direct oxidation of the excipients themselves (e.g., the autoxidation of polysorbates).[8,9] These oxidation reactions generally involve complicated mechanisms. Oxidation reactions sometimes generate unfavorable degradation products, such as hydroperoxide, aldehyde, and epoxide forms,[10,11] which have structural features that may be linked to mutagenicity and carcinogenicity.[12,13] Therefore, oxidation is associated with a high risk of generating potential genotoxic impurities.

An oxidative stressing system, which involves a well-defined oxidation mechanism, can identify realistic oxidation products in advance and is useful for determining the oxidation mechanism if the degradation products correspond to those generated during the storage of the actual drug. Furthermore, the data obtained are helpful for developing strategies to prevent or mitigate the risk of impurities,

Additional Supporting Information may be found in the online version of this article. Supporting Information

Correspondence to: Eiji Ueyama (Telephone: +81-463-31-6888; Fax: +81-463-38-3944; E-mail: ueyama.eiji.s2@daiichisankyo.co.jp)

Journal of Pharmaceutical Sciences, Vol. 102, 104–113 (2013)

such as improving the manufacturing process, formulating an antioxidant, or packaging drugs with an oxygen scavenger. Therefore, pharmaceutical companies have made efforts to develop oxidative stressing systems that predict oxidation products that may be generated during drug storage. Such stressing systems are used to evaluate drug candidates during the early drug development stage.

The literature available regarding approaches for studying oxidation mechanisms is extensive.[14–20] Indeed, these approaches have been used in the pharmaceutical industry, and in many cases, the data obtained about oxidative decomposition have been helpful in the drug development process. However, many of the oxidative stressing systems that have been developed are solution based. Although such systems can be useful, they may not necessarily be reflective of the oxidation reactions that occur in the solid state. Therefore, we are currently developing a solid-based oxidative stressing system that can be applied to the prediction of oxidation products generated in pharmaceutical solids (manuscript in preparation).

Model drugs with known oxidation mechanisms are necessary for the development of a solid-based oxidative stressing system. A triazole antifungal agent, CS-758, 4-[(1*E*,3*E*)-4-[*trans*-5-[[(1*R*,2*R*)-2-(2,4-di-fluorophenyl)-2-hydroxy-1-methyl-3-(1*H*-1,2,4-triazol-1-yl) propyl]thio]-1,3-dioxan-2-yl]-1,3-butadienyl]-3-fluorobenzonitrile (Fig. 1), was the target compound in the present study. This drug has a broad antifungal spectrum covering *Aspergillus* sp. and fluconazole-resistant *Candida* sp., as well as a good safety profile.[21] However, CS-758 shows chemical instability when its crystal is disordered, and characteristic oxidative degradates are generated. This report describes investigations conducted to determine the oxidative degradation pathway of one of the model compounds used in a solid-based oxidative stressing system that is under development.

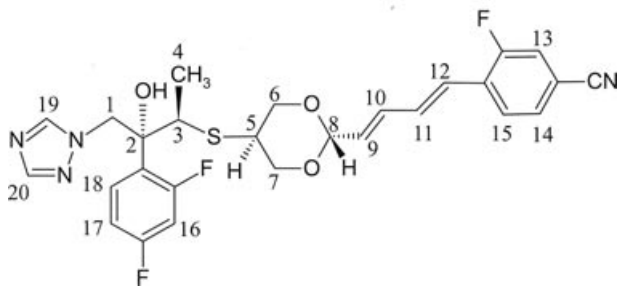

Figure 1. Chemical structures of CS-758 (parent).

MATERIALS AND METHODS

Materials

CS-758 was provided by Daiichi-Sankyo (Tokyo, Japan). All water used was purified using Milli-Q Gradient A10 system (Millipore, Milford, Massachusetts). The oxygen scavenger Sequl® BP-100 was kindly donated by NISSO JUSHI (Ibaraki, Japan). All other chemicals were of analytical grade and from commercial sources.

Preparation of Amorphous Sample using the Grinding Method

The drug substance was ground using a vibrational mill (RM-201; Mitsubishi Chemical Engineering, Tokyo, Japan) for a total of 120 min. The sample was cooled down by occasional refrigeration to prevent melting. The powder X-ray diffraction pattern of the ground sample showed a halo pattern, and the disappearance of the diffraction peaks implied that the drug substance had become amorphous (data not shown). The purity of the amorphous drug sample was greater than 98%, as determined by high-performance liquid chromatography (HPLC) analysis.

Analytical HPLC Conditions

Agilent 1200 and 1100 systems (Agilent Technologies, Waldbronn, Germany) equipped with a photodiode array (PDA) detector were used for HPLC analysis. A YMC Pack Pro C18 [150 × 3.0 mm^2 internal diameter (i.d.); particle size, 3 μm; YMC, Kyoto, Japan) was used as an analytical column, and the temperature of the column was kept at 40°C. The eluent was monitored at a wavelength of 220 nm. Mobile phases A and B were 5 mM ammonium hydrogen carbonate and acetonitrile, respectively. The gradient elution was conducted as follows: from 0 to 12 min, the composition of mobile phase B was increased from 50% to 74%; from 12 to 16 min, its composition was increased from 74% to 90%, and then maintained for 4 min at a constant flow rate of 0.5 mL/min. The injection volume was 5 μL.

Preparative Liquid Chromatography Conditions

Isolation of the degradates was performed using an Agilent 1200 preparative liquid chromatography (LC) system and an EZ-2 Plus solvent evaporator (Genevac, Ipswich, UK). A YMC Pack Pro C18 (150 × 10 mm^2 i.d.; particle size, 5 μm; YMC) was used for separation. Other chromatographic conditions were the same as those used for analytical HPLC with the following exceptions: (a) the flow rate was 5 mL/min, (b) the injection volume was 900 μL, (c) the column temperature was ambient, and (d) for the separation of degradates SS-D6 and SS-D7, methanol was used as mobile phase B.

Liquid Chromatography–Mass Spectrometry Conditions

LC–mass spectrometry (LC–MS) and LC–tandem mass spectrometry (LC–MS/MS) analyses were

performed using an Agilent 1200 system equipped with an LTQ Orbitrap XL mass spectrometer (Thermo Fisher Scientific, Waltham, Massachusetts). The HPLC conditions were the same as the analytical HPLC conditions described previously. For online hydrogen–deuterium (H/D) exchange LC–MS analyses, deuterium oxide was used as a solvent for the preparation of mobile phase A. Electrospray ionization in positive polarity mode was utilized except in the case of Acid-D2 detection, for which atmospheric pressure chemical ionization in negative polarity mode was used.

Nuclear Magnetic Resonance

Nuclear magnetic resonance (NMR) experiments were conducted using an Avance 400 MHz NMR spectrometer (Bruker, Billerica, Massachusetts) equipped with a broadband inverse 5 mm probe. All spectra were acquired from isolated samples dissolved in dimethylsulfoxide-*d6* (DMSO-*d6*) or acetone-*d6*. NMR experiments were performed at 25°C. Chemical shifts are reported in parts per million (ppm) relative to DMSO-*d6* (2.50 ppm) or acetone-*d6* (2.05 ppm). All spectra were recorded in spinning mode. Two-dimensional techniques, including double-quantum filter correlation spectroscopy (DQF-COSY), edited-heteronuclear single-quantum correlation (edited-HSQC) spectroscopy, and heteronuclear multiple-bond correlation (HMBC) spectroscopy were used to establish the H—H network and the C—H, C—C—H, and C—C—C—H connectivity, respectively.

Preparation of Degradates in Solution

Approximately 10 mg of the drug was placed in a glass bottle and dissolved in 8 mL of a dilute solution (a mixture of acetonitrile and water 7:3, v/v). After 2 mL of a 0.5 M HCl solution was added, the sample was stored at 25°C for 1 h. A second sample was prepared in exactly the same manner, except that 2 mL of a 0.5 M NaOH solution was added instead of the 0.5 M HCl solution, and the sample was stored at 25°C for 24 h. A third sample was also prepared in exactly the same manner, except that 2 mL of a 2.5% (w/w) H_2O_2 solution was added instead of the 0.5 M HCl solution, and the sample was stored at 60°C for 1 h. A fourth sample was prepared by placing approximately 22 mg of the drug and 6.5 mg of 2-2′-azobisisobutyronitrile (AIBN) in a glass bottle, and dissolving the sample in 20 mL of acetonitrile. The solution was then stored at 40°C for 1 week.

After the degradates were isolated using a preparative LC, isolated fractions were collected, combined, and evaporated to obtain solid samples. A portion of the solid samples was analyzed using the analytical HPLC method and the chromatographic purity of the samples was confirmed. The compound identification before, and following, isolation was conducted using LC–PDA [retention time and online ultraviolet (UV) spectrum], LC–MS (*m/z*), and LC–MS/MS (fragmentation pattern) analyses.

Preparation of Amorphous Sample Degradates

Amorphous samples were placed in a headspace glass vial that was closed with a cap. The sample was stored in an oven at 50°C for 4 weeks.

After the degradates were isolated by preparative LC, isolated fractions were collected, combined, and evaporated to obtain solid samples. A portion of the solid samples was analyzed by the analytical HPLC method, and the chromatographic purity of the samples was confirmed. The compound identification before, and following, isolation was conducted using LC–PDA (retention time and online UV spectrum), LC–MS (*m/z*), and LC–MS/MS (fragmentation pattern) analyses.

We preliminarily confirmed that sample stability was not easily affected by environmental humidity by conducting comparative stress testing at 40°C (close) and 40°C/75% RH (open). Because the effect of humidity on the stability of samples was slight, humidity was not considered as a factor in the storage of samples during this study.

Preparation of Antioxidant Mixture Samples by the Solvent Evaporation Method

A total of 0.5 g of CS-758 and 0.005 g of antioxidants such as butylated hydroxytoluene (BHT), propyl gallate, and ascorbic acid (100:1, w/w) were dissolved in a mixture of acetone and ethanol (2:1, v/v). The solvent was removed at 30°C under reduced pressure using a rotary evaporator for 2 h. The resultant dried mass was crushed with a spatula, and the coarse-grained powder was used as the solid sample. Using the same method, a control sample was prepared by dissolving 0.5 g of CS-758 into the solvent mixture, then evaporating the solvent. These samples were then stored for up to 2 weeks in a 50°C oven. Aliquots of the sample were collected at specific intervals, dissolved in a diluent, and analyzed using analytical HPLC.

Because the concentration of the drug in samples changes over time as a result of both oxidation and thermolysis, including the formation of other minor degradation products, first-order kinetic theory is not adequate for evaluating oxidative degradation in this case. However, as the degradation apparently follows first-order kinetic theory in this 2-week time range, we adopted the theory to express relative degradation rate numerically.

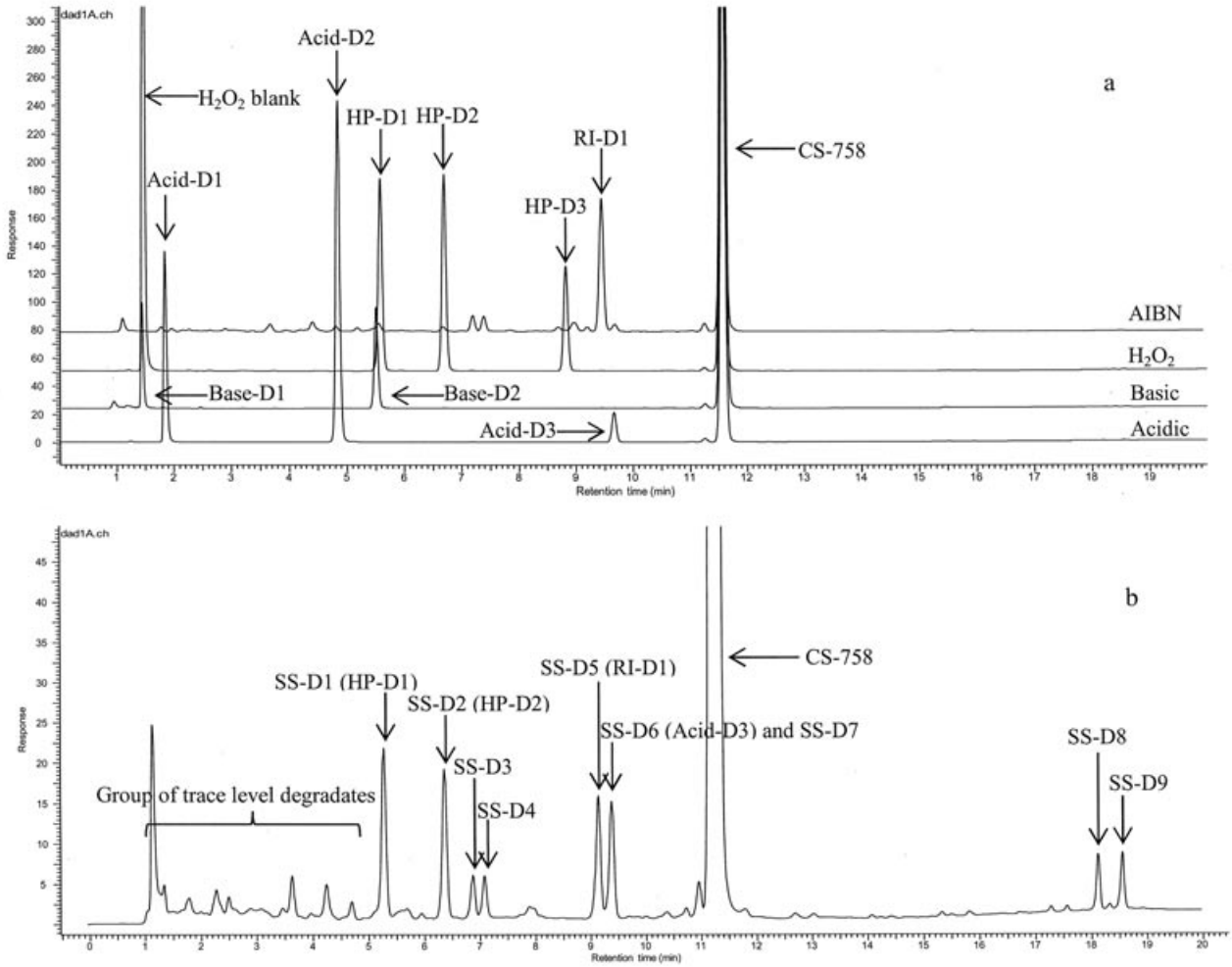

Figure 2. HPLC chromatograms (UV 220 nm) showing degradation profiles of CS-758 (a) overlaid chromatogram obtained from various forced degradation conditions in solution; (i) 0.1 N HCl at 25°C for 1 h, (ii) 0.1 N NaOH at 25°C for 24 h, (iii) 0.5% (w/w) H_2O_2 at 60°C for 1 h, (iv) 2 mM AIBN in acetonitrile at 40°C for 1 week, and (b) chromatogram obtained from a stressed amorphous (120 min grinded drug substance) under the condition at 50°C for 3 weeks.

RESULTS

Profile of Degradates

CS-758 was subjected to acidic, basic, and oxidative conditions in solution. The data obtained from HPLC analysis showed that eight major degradates were generated under these stressing conditions (Fig. 2a). Analytical HPLC showed that the acid degradates, Acid-D1 and -D2, eluted at relative retention times (RRTs) 0.16 and 0.42, respectively; the base degradates, Base-D1 and -D2, eluted at RRTs 0.13 and 0.47, respectively; the H_2O_2 degradates, HP-D1, -D2, and -D3, eluted at RRTs 0.49, 0.59, and 0.77, respectively; and the radical-initiator degradate RI-D1 eluted at RRT 0.82.

The nine degradates generated in the solid state, namely SS-D1, -D2, -D3, -D4, -D5, -D6, -D7, D-8, and -D9, eluted at RRTs of 0.49, 0.59, 0.61, 0.64, 0.82, 0.84, 0.84, 1.58, and 1.64, respectively (Fig. 2b).

High-performance liquid chromatography–PDA and LC–MS data indicated that SS-D6 and SS-D7 were not separated in the preparative and analytical HPLC conditions (Fig. 2b). Therefore, an alternative HPLC method was investigated to separate SS-D6 and SS-D7. The mobile phase pH did not affect the separation status; however, the addition of methanol to the mobile phase resulted in better separation. When mobile phase B was replaced with methanol, SS-D6 and SS-D7 were completely separated with a resolution of 3.4. To accomplish the isolation, SS-D6 and SS-D7 were isolated as a mixture fraction using the acetonitrile-based preparative LC method. The mixture was then separated and isolated via the methanol-based preparative LC method.

Characterization of Degradates in Solution

The results of the LC–MS analyses are summarized in Table 1. Accurate mass analysis of the degradates demonstrated that a resolving power of 60,000 provided the best possible molecular formulas. These formulas were within 5-ppm error of the theoretical molecular weight. Structure information, including estimated molecular formulae, number of active hydrogen atoms, MS/MS fragmentation (the proposed MS/MS fragmentation of CS-758 and its degradates are shown in Supporting Information-1), and λ_{max} of the online UV spectrum led to the proposal of reasonable structures for these degradates (Fig. 3a).

Full assignment of ^{1}H-NMR of RI-D1, the major oxidation product that was also generated in the solid state, is provided in Supporting Information-2. NMR indicated that RI-D1 was similar to the parent compound except at positions 9, 10, 11, and 12, which were located in the dien moiety. The proton–proton correlation of the moiety was identical to that of the parent compound, but the chemical shifts of the protons and carbons at positions 9 and 10 were drastically shifted to a high magnetic field (proton: 3.20 and 3.73 ppm, carbon: 59.1 and 54.7 ppm). This indicated that the methine moiety changed from CH= to >CH. The chemical shifts of the protons and carbons at positions 9 and 10 were consistent with the attachment of oxygen atoms at these positions. Furthermore, accurate mass data suggested that the molecular weight of RI-D1 was 16 amu greater than CS-758, which corresponds to the weight of one additional oxygen atom. Online H/D exchange LC–MS analysis of RI-D1 and CS-768 indicated no difference in the number of active hydrogen atoms in each compound. The online UV–PDA spectrum demonstrated that the absorption maximum (λ_{max}) of R1-D1 shifted to a shorter wavelength relative to that of CS-768. These results support the substitution of an oxygen at this position, as shown in the epoxide structure proposed in Figure 3a. Likewise, data from all analysis types supported the structures proposed for the other degradates (full NMR spectrum assignments are provided in Supporting Information-2). The proposed hydrolysis and oxidation pathways for the creation of these degradates are shown in Figure 3a.

Characterization of Amorphous Sample Degradates

The degradation profile of the amorphous sample differed from those of the acidic and basic conditions (Fig. 2). However, several of the degradates were consistent with those generated under oxidative conditions created by AIBN and H_2O_2 (RI-D1, HP-D1, and HP-D2). SS-D3, SS-D4, SS-D6, SS-D7, SS-D8, and SS-D9 could not be matched to degradates that were generated in any of the forced solution-based degradation conditions. The LC–MS results suggested that

Table 1. Results of LC–MS Analyses

Target	MS Data (*m/z*)	Proposed Molecular Formulae	Error (ppm)	Loss/Gain from CS-758		Active Hydrogen Atoms	Online UV Spectrum λ_{max} (nm)
				Loss	Gain		
CS-758	543.1662	$C_{27}H_{25}N_4O_3F_3S$	−1.88	–	–		
Acid-D1	360.1183	$C_{15}H_{19}N_3O_3F_2S$	−1.41	$C_{12}H_6NF$	–	3	262
Acid-D2	201.0584	$C_{12}H_8NOF$	−0.08	$C_{15}H_{17}N_3O_2F_2S$	–	0	323
Base-D1	561.1752	$C_{27}H_{27}N_4O_4F_3S$	−4.55	–	H_2O	3	296
Base-D2	562.1591	$C_{27}H_{26}N_3O_5F_3S$	−4.47	N	HO_2	2	300
HP-D1 (=SS-D1)	559.1610	$C_{27}H_{25}N_4O_4F_3S$	−2.01	–	O	1	302
HP-D2 (=SS-D2)	559.1609	$C_{27}H_{25}N_4O_4F_3S$	−2.23	–	O	1	302
HP-D3	575.1562	$C_{27}H_{25}N_4O_5F_3S$	−1.50	–	O_2	1	300
RI-D1 (=SS-D5)	559.1603	$C_{27}H_{25}N_4O_4F_3S$	−3.22	–	O	1	272
SS-D3	559.1600	$C_{27}H_{25}N_4O_4F_3S$	−3.76	–	O	2	318
SS-D4	559.1602	$C_{27}H_{25}N_4O_4F_3S$	−3.43	–	O	2	318
SS-D6	543.1652	$C_{27}H_{25}N_4O_3F_3S$	−3.68	–	–	1	302
SS-D7	559.1597	$C_{27}H_{25}N_4O_4F_3S$	−4.31	–	O	1	240
SS-D8	1085.3254	$C_{54}H_{50}N_8O_6F_6S_2$	−1.67	–	$C_{27}H_{25}N_4O_3F_3S$	2	274
SS-D9	1085.3282	$C_{54}H_{50}N_8O_6F_6S_2$	0.92	–	$C_{27}H_{25}N_4O_3F_3S$	2	274

DOI 10.1002/jps

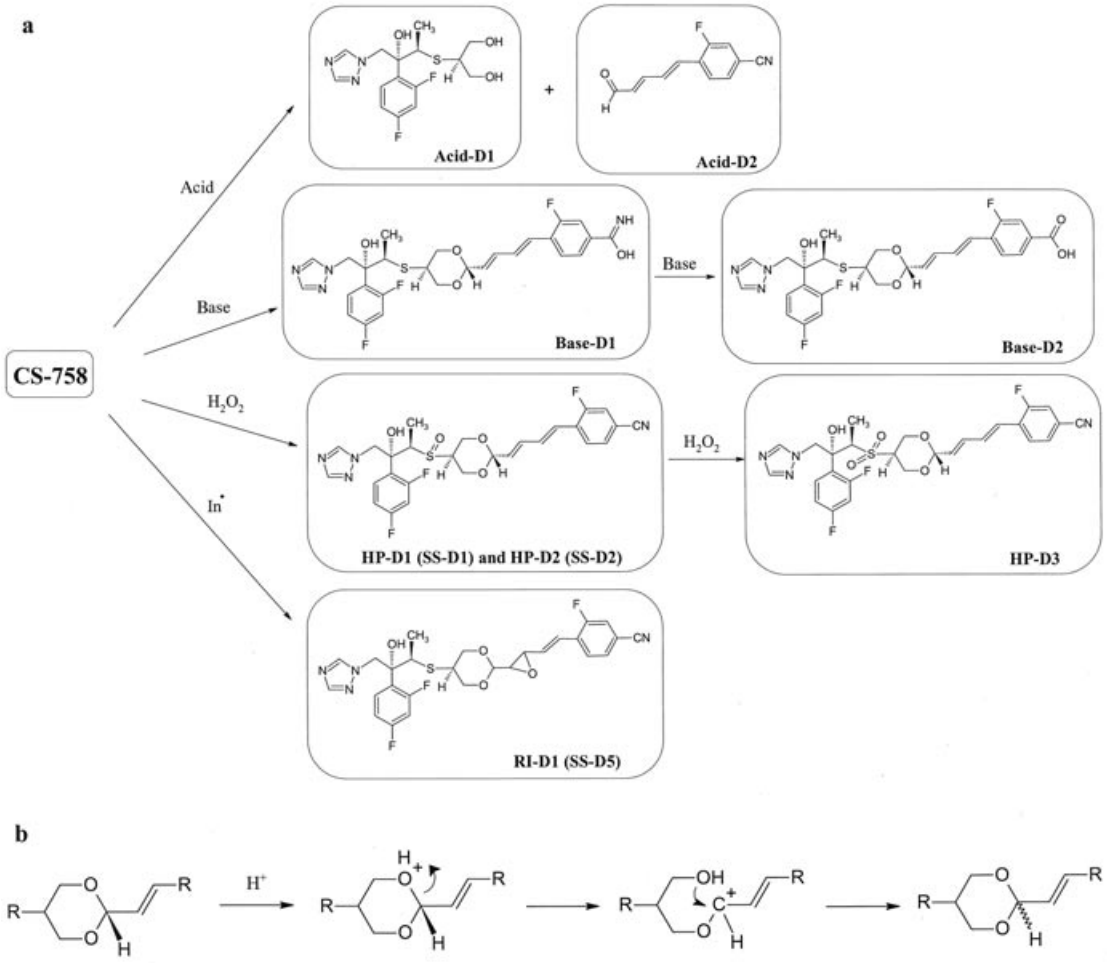

Figure 3. Chemical structures of degradates and degradation pathway in solution state. (a) Main degradation pathway in acid, base, and oxidation condition in solution. (b) Acid-catalyzed epimerization mechanism.

SS-D3, -D4, and -D7 might be simple oxidation products (parent + 16 amu), whereas SS-D6 appeared to be an isomer of the parent. The molecular weights of SS-D8 and -D9 indicated that they might be dimer compounds (Table 1).

Given that SS-D3 and SS-D4 had the same spectroscopic properties, these degradates might be diastereomer compounds of each other. The NMR data showed the disappearance of the methine proton resonance at position 8, and the multiplicity of the resonance at position 9 was changed from double doublet to doublet in comparison with those of CS-768. HMBC data showed that the protons at positions 7 (or 6 in the case of its diastereomer) and 9 correlated with a characteristic carbon downfield at 167 ppm. The chemical shift of the carbon was attributed to a carbonyl carbon located in the adjacent positions at 7 (or 6) and 9. In addition, the edited-HSQC data indicated that the two carbons at positions 6 and 7 were changed to nonequivalent carbons. These results are supportive of dioxane ring-opening hydroxyl forms (Fig. 4).

The LC–MS analyses and NMR data, including the ^{1}H, DQF-COSY, edited-HSQC, and HMBC results, also suggested that SS-D6 was an epimer of the parent. Epimerization may occur at position 8 due to the proposed autoxidation pathway (Fig. 4). However, it was not possible to fully characterize the structure of SS-D6 from these spectroscopic analyses alone. Interestingly, this same degradate was also generated under acidic conditions as a minor degradate (Fig. 2a, at 9.7 min). The main degradation pathway that occurred under acidic conditions involved acid-catalyzed dioxane ring-opening hydrolysis. In this pathway, a hydroxyl group, which was generated via the ring-opening reaction under acidic conditions, carries out a nucleophilic attack on the carbocation at position 8 to form an epimer. Intramolecular recyclization may have occurred under acidic conditions. The proposed acid-catalyzed epimerization mechanism is shown in Figure 3b and the structure of the epimer is supported from the viewpoint of the acid-catalyzed epimerization reaction.

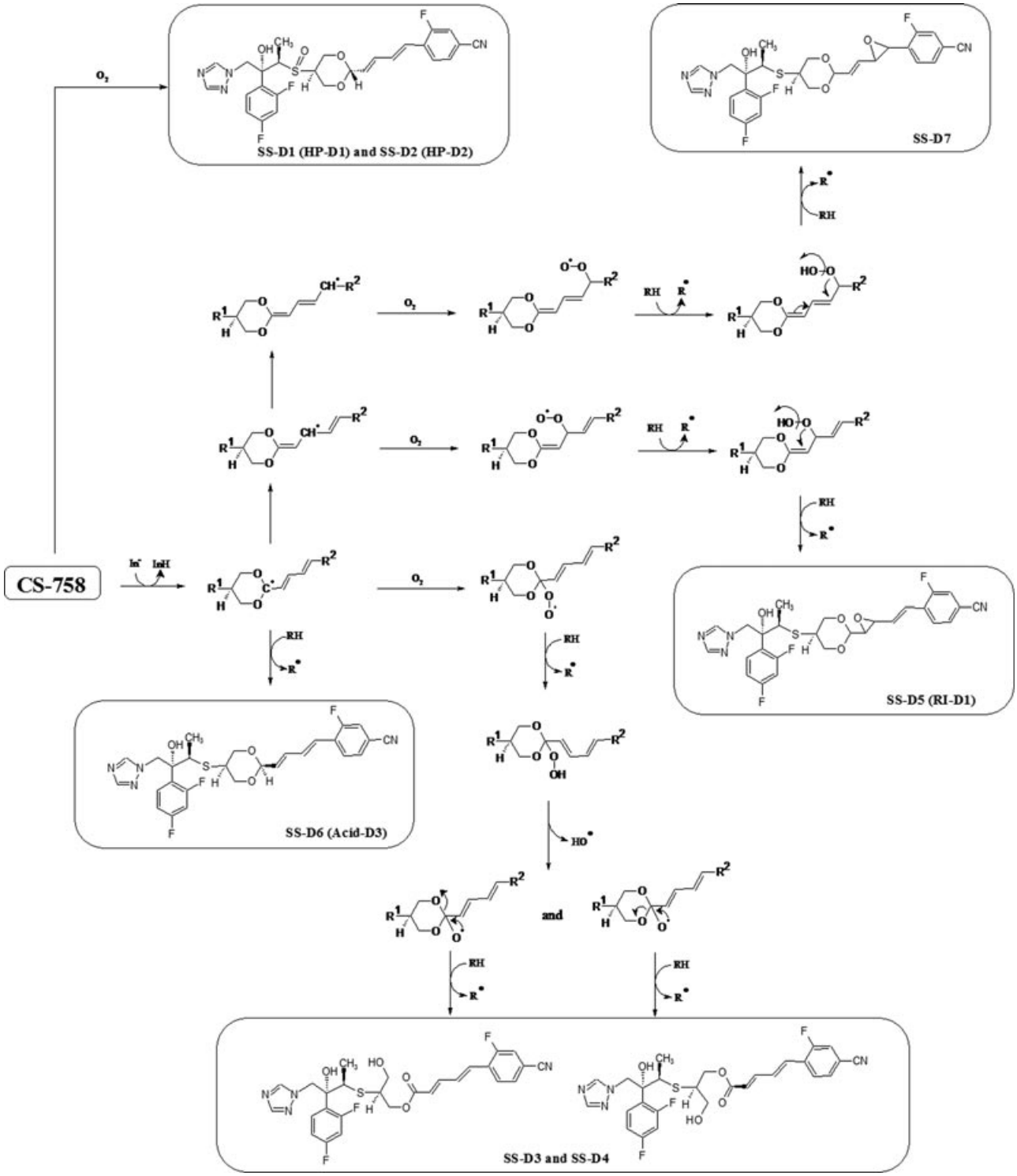

Figure 4. Chemical structures of degradates and proposed oxidation pathway in solid state.

The NMR data (Supporting Information-2) indicated that SS-D7, like RI-D1, showed similarity in structural resonances to the parent compound, except at positions 9, 10, 11, and 12. The chemical shifts of the protons and carbons at positions 11 and 12 were significantly shifted to high magnetic field in comparison with those of CS-768. The LC–MS, online UV–PDA, and NMR data supported the substitution of oxygen at positions 11 and 12, as shown in the proposed epoxide structure (Fig. 4).

SS-D8 and SS-D9 (Fig. 5) were considered to be diastereomers of each other, as these degradates had the same spectroscopic properties. The NMR data showed similarity in the structural resonances between these compounds and the parent compound, except at positions 9, 10, 11, and 12. In the case of

 DOI 10.1002/jps

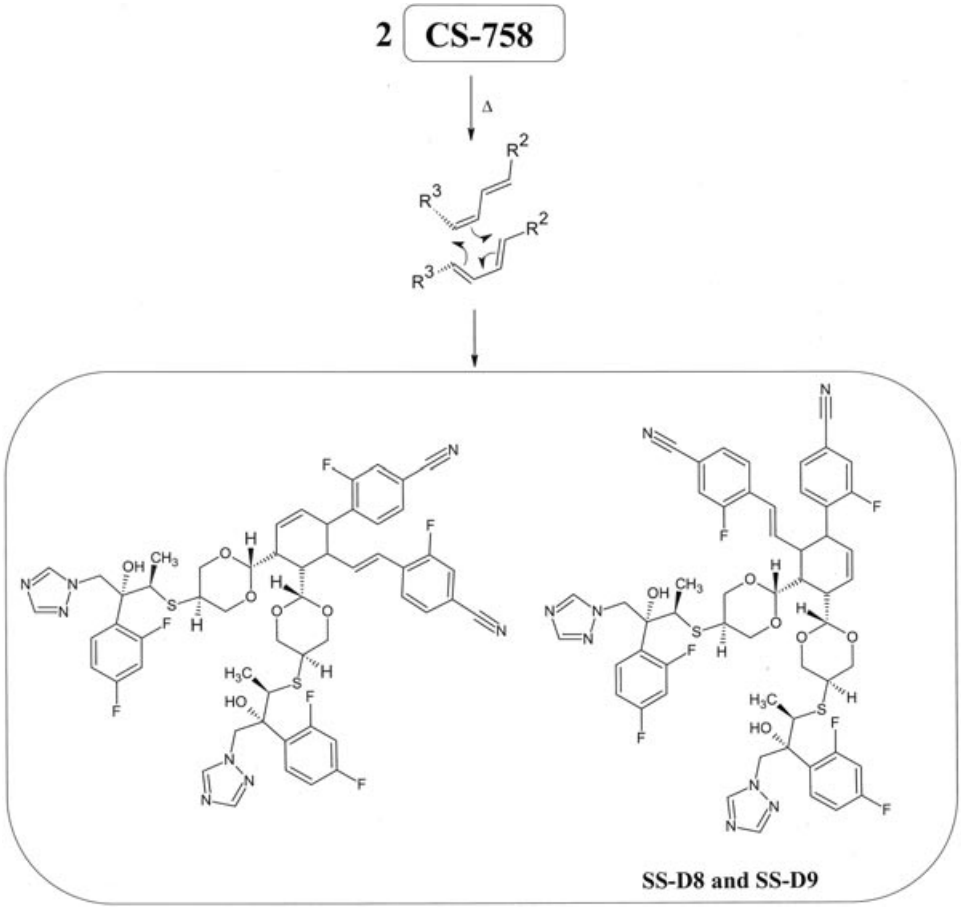

Figure 5. Chemical structures of degradates and proposed thermolysis pathway in solid state.

SS-D8, DQF-COSY indicated key correlations of H-9 (2.17−2.22 ppm) to H-9′ (2.84 ppm), and of H-10 (3.08−3.14 ppm) to H-12′ (4.09−4.11 ppm), through H−H connectivity; HMBC also showed reasonable key correlations that supported the proposed structure. The key correlations confirmed the presence of a six-member cyclic ring. Furthermore, edited-HSQC data confirmed that positions 11, 12, 10′, and 11′ were part of the methylidene group (−CH=). All of the correlations observed in the DQF-COSY, edited-HSQC, and HMBC experiments confirmed the proposed structures of SS-D8 and SS-D9.

DISCUSSION

Degradation Mechanism

Most degradation of amorphous samples likely occurs via oxidation, as most of the degradates are oxidation products. Proposed solid-state degradation pathways that lead to the measured degradates are presented in Figures 4 and 5. The oxidation pathway presented in Figure 4 involves radical-mediated oxidation (autoxidation), in which a hydrogen atom is abstracted from the methine carbon adjacent to the dien moiety to form a delocalized vinylic radical intermediate, with molecular oxygen being subsequently added to the radical position to form hydroperoxides. On the basis of the proposed autoxidation pathway, three oxidation routes can be envisioned that lead to the generation of the dioxane ring-opening hydroxyl forms (SS-D3 and -D4), the 9,10-epoxide form (SS-D5), or the 11,12-epoxide form (SS-D7), depending on the substituted position of molecular oxygen. Furthermore, the generation of the epimer compound (SS-D6) provides strong support for the proposed initiation step. If the delocalized vinylic radical intermediates are generated before the addition of the oxygen molecule, the generation of 8,10-dien and 8,11-dien degradates would be expected in addition to SS-D6 (9,11-dien). However, 8,10- and 8,11-dien degradates were not confirmed as primary degradation products. Because it is difficult for an 8-en structure to take a chair conformation, a relatively sterically stable form of dioxane ring, it is harder to generate than 9,11-dien.

The proposed degradation mechanism was confirmed from two perspectives: (1) the stability of the amorphous sample in an anaerobic condition and (2) the effect of antioxidants on the rate of oxidation. When the amorphous sample was stressed under an

Table 2. Effect of Antioxidants on CS-758 Chemical Stability

Antioxidant	Mechanism	k ($\times 10^3$ day^{-1})	Relative Rate Constant
Ascorbic acid	Acid, preferentially oxidized	3.852	0.77
Propyl gallate	H-atom donor	1.129	0.23
Butylated hydroxytoluene	H-atom donor	0.479	0.10
Additive free (control)	–	5.006	1.00

anaerobic condition that was created using an oxygen scavenger, the generation of all oxidation degradates was inhibited. The results of stressing the amorphous compound by storage at 50°C with or without an oxygen scavenger for up to 4 weeks are shown in Supporting Information-3. Furthermore, the addition of antioxidants to the amorphous sample decreased the oxidation rate (Table 2; the kinetic plot is shown in Supporting Information-4). The effectiveness of the antioxidants was ranked by the relative rate constant: BHT > propyl gallate > ascorbic acid > control. These results suggest that the CS-758 radical species mediates the oxidation reaction in the amorphous sample because BHT and propyl gallate, which act as radical scavengers (H-atom donors), competitively prevented oxidation.

In contrast, the generation of SS-D8 and SS-D9 was not prevented by the addition of any antioxidants or by storage under an anaerobic condition. This suggests that these degradates were not oxidation products, but products of thermolysis. We proposed a Diels–Alder reaction as the chemical degradation pathway (Fig. 5), with the generation rate dependent on temperature. This reaction mechanism provides a possible explanation for the empirical observation that the generation of SS-D8 and SS-D9 was not prevented by the addition of antioxidants or by storage under an anaerobic condition. In addition, the LC–MS results showed that two minor peaks, which were eluted in the range of 17–18 min on the chromatogram shown in Figure 2, have the same *m/z* as SS-D8 and SS-D9. The molecular weights of these minor peaks indicated that they might be other dimer compounds. Although these minor peaks were not isolated, these compounds may be Diels–Alder reaction products of the C11–C12 double bond with the 9,11-dien moiety. There may have been a sterical restriction that prevented large quantities of these products from forming.

In the initiation step of the proposed oxidation mechanism (Fig. 4), the hydrogen atom at position 8 is abstracted by some foreign element. Although the true foreign element that initiates the autoxidation remains unknown, heat, trace impurities (e.g., radical initiators, peroxides, or transition metals), or mechanoradicals generated by mechanical forces[22] is possible initiator elements.

In conclusion, the degradates of the triazole antifungal agent CS-758, both in solution and in solid state, were characterized. Radical-mediated oxidation (autoxidation) was proposed as the main degradation pathway in the solid state. The initiation step of this oxidation reaction was hydrogen atom abstraction from the methine carbon adjacent to the dien moiety to form a delocalized vinylic radical intermediate. Molecular oxygen was subsequently added to the radical position to form hydroperoxides. On the basis of the proposed autoxidation pathway, three oxidation routes were envisioned that lead to the generation of characteristic oxidation products, depending on the substituted position of molecular oxygen. Furthermore, the generation of the epimer compound (SS-D6) provided strong support for the proposed initiation step. The H-atom donor-type antioxidants, BHT, and propyl gallate, as well as the oxygen scavenger, significantly reduced the rate of oxidation, suggesting that the drug radical species mediates the oxidation reaction in the amorphous form (autoxidation). The knowledge acquired on the degradation pathway of this model compound is useful for the development of an oxidative stressing system, which is currently under investigation.

ACKNOWLEDGMENTS

The authors would like to thank Daiichi Sankyo Company for encouraging publication of this work.

REFERENCES

1. Baertschi SW, Brunner H, Bunnell CA, Cooke GG, Diseroad B, Dorman DE, Jansen PJ, Kemp CA, Maple SR, McCune KA, Speakman JL. 2008. Isolation, identification, and synthesis of two oxidative degradation products of olanzapine (LY170053) in solid oral formulations. J Pharm Sci 97:883–892.
2. Ueyama E, Takahashi F, Ohashi J, Konse T, Kishi N, Kano K. 2012. Mechanistic study on degradation of azelnidipine solution under radical initiator-based oxidative conditions. J Pharm Biomed Anal 61:277–283.
3. Dyakonov T, Muir A, Nasri H, Toops D, Fatmi A. 2010. Isolation and characterization of cetirizine degradation product: Mechanism of cetirizine oxidation. Pharm Res 27:1318–1324.
4. Hartauer KJ, Arbuthnot GN, Baertschi SW, Johnson RA, Luke WD, Pearson NG, Rickard EC, Tingle CA, Tsang PK, Wiens RE. 2000. Influence of peroxide impurities in povidone and crospovidone on the stability of raloxifene hydrochloride in tablets: Identification and control of an oxidative degradation product. Pharm Dev Technol 5:303–310.
5. Hong J, Lee E, Carter JC, Masse JA, Oksanen DA. 2004. Antioxidant-accelerated oxidative degradation: A case study of transition metal ion catalyzed oxidation in formulation. Pharm Dev Technol 9:171–179.

6. Seburg RA, Ballard JM, Hwang TL, Sullivan CM. 2006. Photosensitized degradation of losartan potassium in an extemporaneous suspension formulation. J Pharm Biomed Anal 42:411–422.
7. Qin X, Frech P. 2001. Liquid chromatography/mass spectrometry (LC/MS) identification of photooxidative degradates of crystalline and amorphous MK-912. J Pharm Sci 90:833–844.
8. Yao J, Dokuru DK, Noestheden M, Park SS, Kerwin BA, Jona J, Ostovic D, Reid DL. 2009. A quantitative kinetic study of polysorbate autoxidation: The role of unsaturated fatty acid ester substituents. Pharm Res 26:2303–2313.
9. Kerwin BA. 2008. Polysorbates 20 and 80 used in the formulation of protein biotherapeutics: Structure and degradation pathways. J Pharm Sci 97:2924–2935.
10. Harmon PA, Biffar S, Pitzenberger SM, Reed RA. 2005. Mechanism of the solution oxidation of refecoxib under alkaline conditions. Pharm Res 22:1716–1726.
11. Boccardi G. 2005. Oxidative susceptibility testing. In Pharmaceutical stress testing: Predicting drug degradation; Baertschi SW, Ed. New York City, New York: Taylor & Francis, pp 205–234.
12. Ball JC, Young WC, Wallington TJ, Japar SM. 1992. Mutagenic properties of a series of alkyl hydroperoxides. Environ Sci Technol 26:397–399.
13. Muller L, Mauthe RJ, Riley CM, Andino MM, Antonis DD, Beels C, DeGeorge J, De Knaep AG, Ellison D, Fagerland JA, Frank R, Fritschel B, Galloway S, Harpur E, Humfrey CD, Jacks AS, Jagota N, Mackinnon J, Mohan G, Ness DK, O'Donovan MR, Smith MD, Vudathala G, Yotti L. 2006. A rationale for determining, testing, and controlling specific impurities in pharmaceuticals that possess potential for genotoxicity. Regul Toxicol Pharmacol 44:198–211.
14. Zhu DA, Zhang GG, George KL, Zhou D. 2011. A novel accelerated oxidative stability screening method for pharmaceutical solids. J Pharm Sci 100:3529–3538.
15. Reynolds DW, Galvani M, Hicks SR, Joshi BJ, Kennedy-Gabb SA, Kleinman MH, Parmar PZ. 2012. The use of N-methylpyrrolidone as a cosolvent and oxidant in pharmaceutical stress testing. J Pharm Sci 101:761–776.
16. Kawaguchi-Murakami Y, Fukutsu N, Kajiro T, Araki T, Murakami T, Kawasaki T, Kishi N, Konno M. 2009. A prediction system of oxidation reaction as a solid-state stress condition: Applied to a pyrrole-containing pharmaceutical compound. J Pharm Biomed Anal 50:328–335.
17. Nelson ED, Harmon PA, Szymanik RC, Teresk MG, Li L, Suburg RA, Reed RA. 2006. Evaluation of solution oxygenation requirements for azonitrile-based oxidative forced degradation studies of pharmaceutical compounds. J Pharm Sci 95:1527–1539.
18. Harmon PA, Kosuda K, Nelson E, Mowery M, Reed RA. 2006. A novel peroxy radical based oxidative stressing system for ranking the oxidizability of drug substances. J Pharm Sci 95:2014–2028.
19. Betiqeri S, Thakur A, Raqhavan K. 2005. Use of 2,2′-azobis(2-amidinopropane) dihydrochloride as a reagent tool for evaluation of oxidative stability of drugs. Pharm Res 22:310–317.
20. Reid DL, Calvitt CJ, Zell MT, Miller KG, Kingsmill CA. 2004. Early prediction of pharmaceutical oxidation pathways by computational chemistry and forced degradation. Pharm Res 21:1708–1717.
21. Kamai Y, Harasaki T, Fukuoka T, Ohya S, Uchida K, Yamaguchi H, Kuwahara S. 2002. In vitro and in vivo activities of CS-758 (R-120758), a new triazole antifungal agent. Antimicrob Agents Chemother 46:367–370.
22. Polizzi MA, Singhal D, Colvin J. 2008. Mechanoradical-induced degradation in a pharmaceutical blend during high-shear processing. Pharm Dev Technol 13:457–462.